



Citation: E.E. Başakın, Ö. Ekmekciöğlü, M. Özger, N. Altınbaş, L. Şaylan (2021) Estimation of measured evapotranspiration using data-driven methods with limited meteorological variables. *Italian Journal of Agrometeorology* (1): 63-80. doi: 10.36253/ijam-1055

Received: August 18, 2020

Accepted: March 21, 2021

Published: August 9, 2021

Copyright: © 2021 E.E. Başakın, Ö. Ekmekciöğlü, M. Özger, N. Altınbaş, L. Şaylan. This is an open access, peer-reviewed article published by Firenze University Press (<http://www.fupress.com/ijam>) and distributed under the terms of the Creative Commons Attribution License, which permits unrestricted use, distribution, and reproduction in any medium, provided the original author and source are credited.

Data Availability Statement: All relevant data are within the paper and its Supporting Information files.

Competing Interests: The Author(s) declare(s) no conflict of interest.

Estimation of measured evapotranspiration using data-driven methods with limited meteorological variables

EYYUP ENSAR BAŞAKIN^{1,*}, ÖMER EKMEKÇİOĞLU¹, MEHMET ÖZGER¹, NİLCAN ALTINBAŞ², LEVENT ŞAYLAN²

¹ *Hydraulics Division, Civil Engineering Department, Istanbul Technical University, Maslak 34469, Istanbul, Turkey*

² *Department of Meteorological Engineering, Faculty of Aeronautics and Astronautics, Istanbul Technical University, Maslak 34469, Istanbul, Turkey*

*Corresponding author. E-mail: basakin@itu.edu.tr

Abstract. Determination of surface energy balance depends on the energy exchange between land and atmosphere. Thus, crop, soil and meteorological factors are crucial, particularly in agricultural fields. Evapotranspiration is derived from latent heat component of surface energy balance and is a key factor to clarify the energy transfer mechanism. Development of the methods and technologies for the aim of determining and measuring of evapotranspiration have been one of the main focus points for researchers. However, the direct measurement systems are not common because of economic reasons. This situation causes that different methods are used to estimate evapotranspiration, particularly in locations where no measurements are made. Thus, in this study, non-linear techniques were applied to make accurate estimations of evapotranspiration over the winter wheat canopy located in the field of Atatürk Soil Water and Agricultural Meteorology Research Institute Directorate, Kırklareli, Turkey. This is the first attempt in the literature which consist of the comparison of different machine learning methods in the evapotranspiration values obtained by the Bowen Ratio Energy Balance system. In order to accomplish this aim, support-vector machine, Adaptive neuro fuzzy inference system and Artificial neural network models have been evaluated for different input combinations. The results revealed that even with only global solar radiation data taken as an input, a high prediction accuracy can be achieved. These results are particularly advantageous in cases where the measurement of meteorological variables is limited. With the results of this study, progress can be made in the efficient use and management of water resources based on the input parameters of evapotranspiration especially for regions with limited data.

Keywords: bowen ratio energy balance, artificial neural network, adaptive neuro fuzzy inference system, winter wheat.

1. INTRODUCTION

Investigation of the relocation of water with events such as precipitation, surface flow, evapotranspiration and infiltration are of great importance for

the management of water resources. Throughout the world, clean water resources are gradually decreasing due to climate change and, most importantly, inadequate management of water resources in agriculture. Sustainable use of water resources is only possible through accurate monitoring of all hydrological cycle elements and utilizing this information for decision support in water resources management. Evapotranspiration (ET) is one of the most important components in hydrological cycle among the others which are precipitation, infiltration, surface and groundwater flow. Evapotranspiration can be described as the change of phase of water in the soil, plants, rivers, lakes and seas with the effect of atmospheric conditions and movement towards the atmosphere. It consists of two factors: evaporation and transpiration. Evaporation represents the conveyance of water from the water surface to the atmosphere, while transpiration accounts for the transmission of water from land to the atmosphere through plants. Evapotranspiration calculations are performed either by direct measurement or indirect methods as well as estimation methods. In this study, the Bowen Ratio Energy Balance (BREB) method was used to measure actual ET and mathematical models have been proposed using the data obtained from the measurements.

Artificial Neural Network (ANN) and Adaptive Neuro Fuzzy Inference System (ANFIS), which are frequently used in many areas in recent years, are also widely used in ET calculations (Wu *et al.*, 2019; Ferreira *et al.*, 2019; Maroufpoor *et al.*, 2020). In addition, new machine learning techniques have been introduced such as support vector machine (SVM), gene expression programming (GEP), extreme learning machine (ELM) and the methods that enable to predict ET have been diversified. Abdullah *et al.* (2015) predicted the reference ET (ET_0) values by using ELM and feedforward backpropagation (FFBP), then compared the results with the values obtained from Penman & Monteith equation (Allen *et al.*, 1998). Besides, they conducted sensitivity analysis with five variables (maximum and minimum air temperature, sunshine hours, relative humidity and wind speed) for 3 different locations. It was pointed out that the sensitivity of the variables was changed according to the location. Estimations were made with different input variations and ELM performance was found to be higher than the FFBP model with higher coefficient of determination ($R^2=0.991$ for ELM and $R^2=0.985$ for FFBP) as well as lower computation time. It has been shown that the solution in the ELM model is almost twice as fast as in the FFBP model. In addition, compared to the estimates made with all inputs, the predictions made with four inputs (without net radiation) are more successful, albeit with a slight difference.

Gocic *et al.* (2016) calculated monthly reference evapotranspiration by using ELM and compared their results with different empirical equations for a 31-year period. Minimum and maximum air temperatures, actual vapor pressure, wind speed and sunshine duration were used as inputs while the empirical equation results as the output. The outputs obtained by three different empirical equations, namely Hargreaves, Priestley–Taylor and Turc, were subjected to correlation analysis with the results of FAO Penman & Monteith equation (FPM). It is stated that the results of the three above mentioned equations have high correlations with FPM. The prediction models were established by separating the dataset as 50% training and 50% testing sets. The model performances were evaluated on the basis of empirical equations and they concluded that the Hargreaves model outperforms to models obtained by with other two equations.

Wen *et al.* (2015) predicted daily evapotranspiration using support vector machines. Predictions were conducted with limited data and the results compared with the values obtained from FAO Penman & Monteith equation. Similar to previous studies in the literature, the model with predominant maximum temperature (T_{max}) and minimum temperature (T_{min}) parameters was also evaluated by comparing with different empirical calculation methods as well as ANN results. In order to avoid dimensional differences in models, normalization was performed on each data set. As a result of the model evaluation, it was stated that SVM model showed superior performance even when the different model structures of ANN were considered. However, although the dominant parameters were expressed as T_{max} and T_{min} , it was found that the predictions made by these two inputs ($R^2=0.772$) performed rather poorly than the predictions made by all inputs ($R^2=0.95$). Similarly, Antonopoulos and Antonopoulos (2017) made predictions with ANN by using limited meteorological variables and compared the results with different empirical methods. Optimum input combination was determined with different input variations. As a result of the normalization of daily data for five years, the results of ANN model and other deterministic models were evaluated by considering the results of the widely accepted Penman & Monteith method. The most appropriate ANN structure (4-6-1) was obtained for the predictions and it was concluded that better predictions can be achieved with a smaller number of variables, e.g. temperature and solar radiation.

With the daily data obtained from the 13 different meteorological stations, Yassin *et al.* (2016) evaluated the performance of ANN and GEP. Reference ET was predicted by using maximum, minimum and mean air

temperatures; maximum, minimum and mean relative humidity, wind speed and global solar radiation. They aimed to improve model performance by using validation set and the calculated ET values by means of Penman & Monteith equation was used as a target value. Furthermore, the ANN model was found to be slightly more successful than the GEP. Nevertheless, GEP can be used in ET calculations in terms of less time consuming, since it gives algebraic equations. In the study, in which the validation phase was also considered during the data set separation, in order to increase the reliability of the model results, Banda *et al.* (2017), predicted reference evapotranspiration by dividing the data set into three as train, validation and test. In their evaluation it is pointed out that multi-layer perceptron (5-5-1) has the highest accuracy, although there is not a big difference between the applied neuro computing techniques. The small difference between the model performances may be due to the normalization process.

In the study comparing tree algorithms, which are one of another machine learning techniques, with SVM results, Fan *et al.* (2018) stated that SVM has higher accuracy than the tree algorithms for different climate conditions, particularly with the limited meteorological data. Ferreira *et al.* (2019) drew attention to regional models rather than local predictions in the calculation of ET_0 . They used the temperature and relative humidity data of 203 stations representing the entire Brazil. For ANN, the previous 2-day and 4-day data were shown to be the best options for generalization capacity in temperature-based and temperature-and relative humidity-based models, respectively. Additionally, the ANN approach was applied to estimate the surface soil temperature by Lazzus (2014) and to determine the harvestable water from air humidity data by Khaledi (2019). Furthermore, Şaylan *et al.* (2017) used ANN and adaptive neuro-fuzzy inference system for modeling of soil water content. Şaylan *et al.* (2019) modeled the surface conductance parameter in Penman & Monteith equation over a crop by ANN. Following the widespread use of mathematical models in the prediction of hydrological parameters, ensemble models are also frequently used in the literature. Ensemble models are used for precipitation (Xu *et al.*, 2020; Ahmed *et al.*, 2020), flood (Tiwari and Chatterjee, 2010; Liu *et al.* 2017) and water quality (Partalas *et al.* 2008; Elkiran *et al.* 2019) predictions. For reference evapotranspiration, Nourani *et al.* 2019 has established both empirical ensemble and artificial intelligence ensemble models with 2 different strategies. They used Feed Forward Neural Network (FFNN), Adaptive Neuro Fuzzy Inference System (ANFIS), Support Vector Regression (SVR) methods for artificial intelligence

ensemble, while Hargreaves and Samani (HS), Modified Hargreaves and Samani (MHS), Makkink (MK) and Ritchie (RT) equations were utilized for the empirical ensembles. They established models to predict reference evapotranspiration with meteorological variables obtained from five different regions, including Turkey. It was concluded that ensemble models have higher accuracy than stand-alone models. In addition, it has been pointed out that artificial intelligence-based ensemble performs better than empirical ensemble models.

As seen above, in many studies, daily total reference evapotranspiration was modeled with nonlinear approaches using daily meteorological data. The difference of this study from other studies is that instead of reference ET, the actual evapotranspiration measured by the BREB method with short time intervals (30-min) is determined for the first time in the literature using data-driven models with a limited number of meteorological variables measured in the same time interval.

Main aim of this study was to estimate the 30-min actual evapotranspiration of winter wheat measured by BREB method as a function of limited number of meteorological variables such as 30-min average air temperature (T), relative humidity (RH), global solar radiation (R_s), vapor pressure deficit (VPD) using data-driven models (SVM, ANFIS and ANN) at the experiment field of Atatürk Soil Water and Agricultural Meteorology Research Institute in the Kırklareli city, locates in the north-west part of Turkey.

2. MATERIALS AND METHODS

2.1. Study area and data

Study area covering 8 ha is located in the field of Atatürk Soil Water and Agricultural Meteorology Research Institute Directorate (41°41'53" N, 27°12'37" E, 171 m asl), in Kırklareli which is one of three provinces located in the Thrace Region, Turkey (Fig. 1). The surface water potential of Kırklareli constitutes 1.2% of the Turkey's surface water, while the amount of economically irrigable land in the province is 112013 ha (Ekmeçyapar and Cebi, 2017). Thus, Kırklareli has a suitable area to observe the agricultural activities. In this study, the observations were taken during the 2009-2010 winter wheat growing period from this area.

The evapotranspiration (obtained from latent heat flux) values were calculated by using Bowen Ratio Energy Balance method by using the following equations (Bowen, 1926).

$$\beta = \gamma \left(\frac{\Delta T}{\Delta e} \right) = \frac{H}{LE} \quad (1)$$

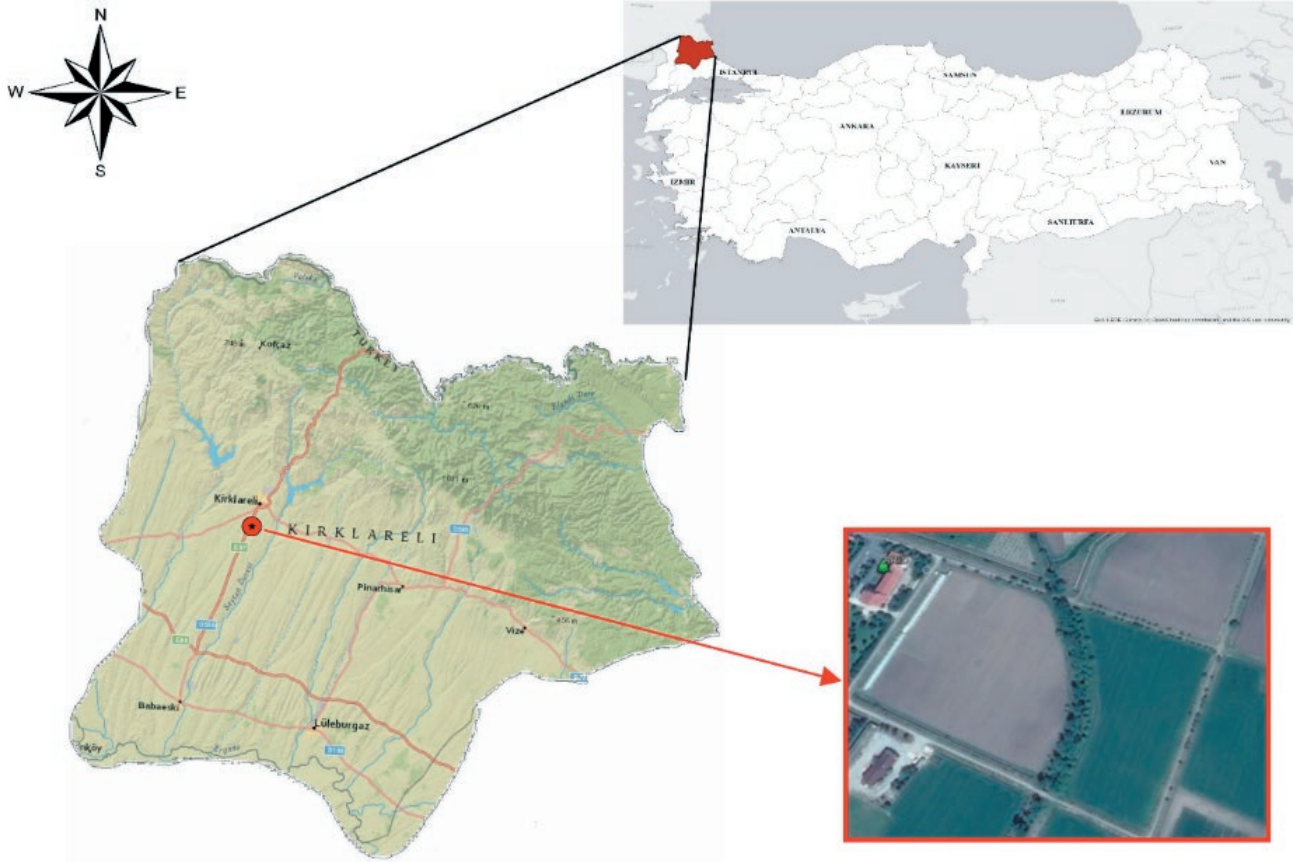


Fig. 1. Study area.

$$R_n - G - LE - H = 0 \quad (2)$$

$$LE = \frac{R_n - G}{(1 + \beta)} \quad (3)$$

where, β is Bowen ratio, is psychrometric constant ($\text{kPa } ^\circ\text{C}^{-1}$), R_n is net radiation (Wm^{-2}); G is soil heat flux (Wm^{-2}); LE is latent heat flux (Wm^{-2}); H is sensible heat flux (Wm^{-2}); ΔT is the temperature gradient ($^\circ\text{C}$) and Δe is the vapor pressure gradient (kPa) over the height interval above canopy surface.

BREB system is built on a 10 m measurement mast. The sensors found in the BREB measurement system and their measurement heights are given in Tab. 1.

Meteorological variables were measured in an interval of 1 s and recorded as an average of 30 minute. In this study, the raw BREB data recorded in every 30-min were used to estimate evapotranspiration. One of the most difficulties in using the BREB method is that the temperature and vapor pressure differences used in calculation of the bowen ratio generally approach -1 near dawn and dusk. Apart from this, the temperature and vapor pressure gradients should be controlled in the

Tab. 1. BREB measurement system components and the measurement heights.

Sensor	Model	Measurement height/depth
Data Logger	Campbell Scientific, CR1000	-
Temperature and Relative Humidity	Vaisala, HMP	2 m and 3m
Wind speed and direction	NRG, RNRG	0.5 m, 1 m, 2 m, 5 m, 10 m
Precipitation	Campbell Scientific, TE	1 m
Global solar radiation	Kipp&Zonen, NR	2 m
Net radiation	Kipp&Zonen, NR	2 m
Soil heat flux	Hukseflux, HFP	8 cm

relationships between H and LE . Therefore, data were checked according to the criteria of Ohmura (1982) and Perez *et al.* (1999) to avoid suspicious data situations. Then, incorrect data were eliminated and miss-

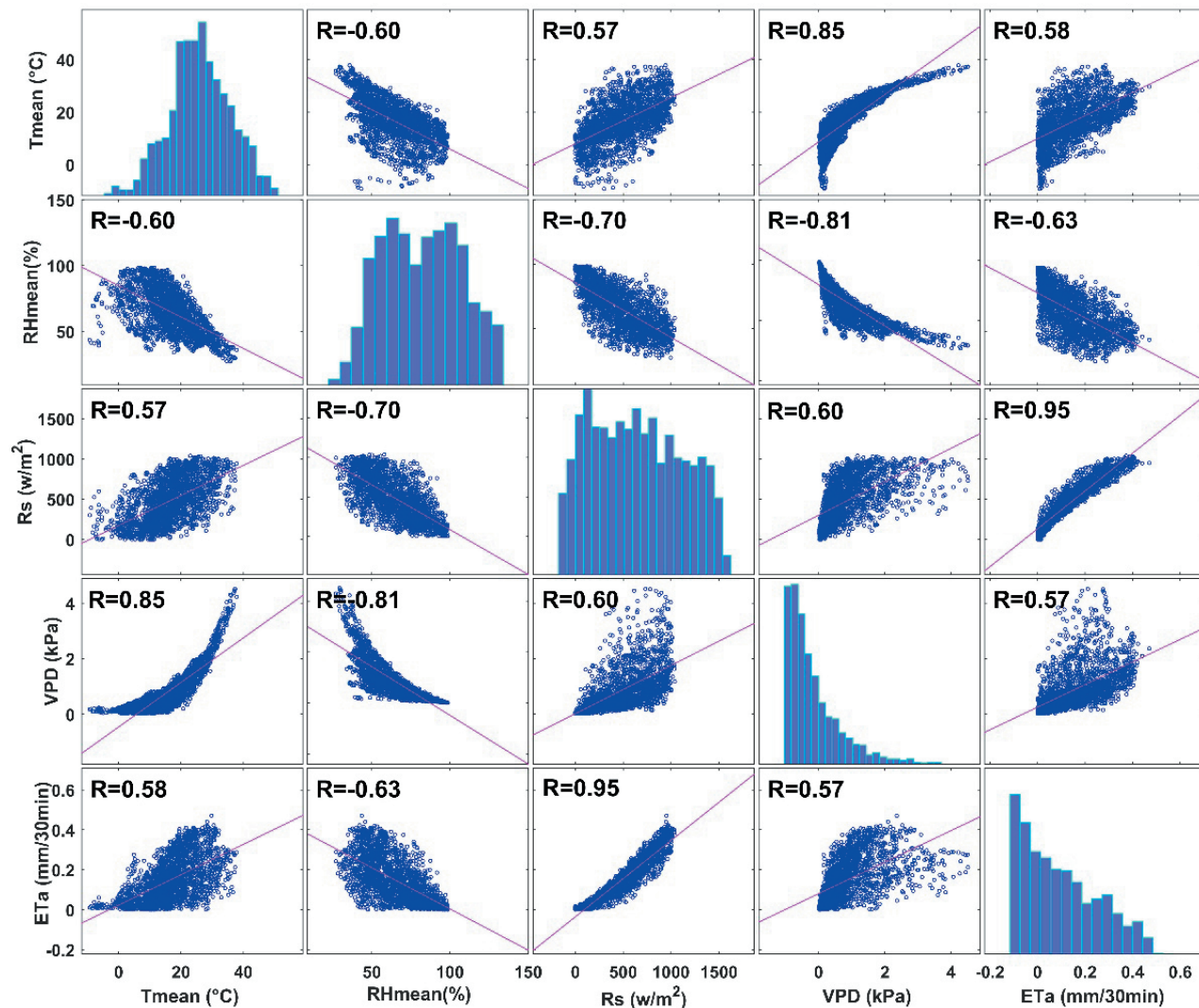


Fig. 2. Correlation matrix.

ing data were completed by considering criteria. During the measurement, various meteorological factors such as global solar radiation, net radiation, humidity and temperature etc. were measured and recorded. However, each measured variable is not included in the models as an input in data driven techniques to ensure the usability of the proposed methods. For instance, net radiation was not included in the model, even though it has considerably high correlation with the actual ET, since it is already calculated by using solar radiation. Additionally, net radiation is not continuously measured data in the world. Therefore, it is considered sufficient to include only global solar radiation in the model to pay regard to easy use of the models. As a result, using these variables, latent heat flux was calculated with the help of Equation

1 to Equation 3 and it is converted from the latent heat flux to the actual evapotranspiration (ET_a). Thus, mean temperature (T), relative humidity (R_H), global solar radiation (R_s) and vapor pressure deficit (VPD) were used as inputs, while actual evapotranspiration was used as the output for the proposed models. The correlation matrix is introduced in Fig. 2. The time-series of the input variables and output are also given in Fig. 3.

As can be seen from the correlation matrix in Figure 2, global solar radiation has the highest correlation with the ET_a among the other input variables. It is followed by relative humidity, which has the negative correlation, mean temperature and vapor pressure deficit, respectively. Considering that global solar radiation shows such a high correlation ($R=0.95$), it is possible that high accu-

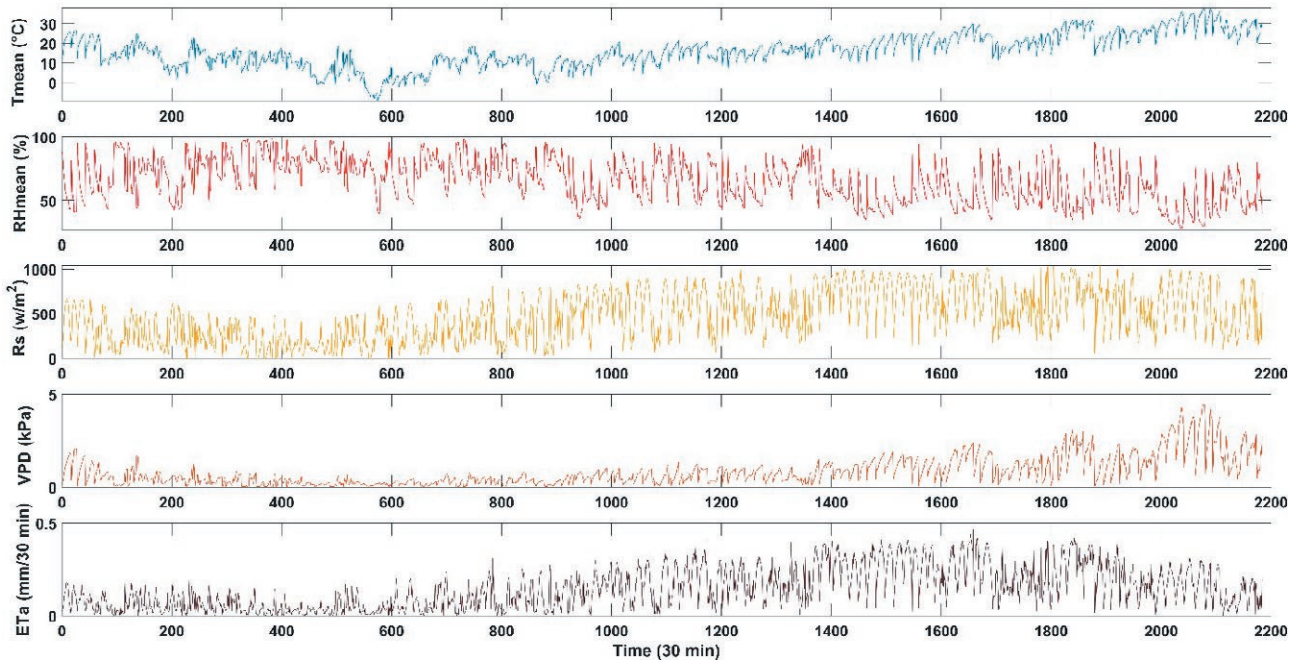


Fig. 3. Time series of the calculated variables with BREB.

Tab. 2. Basic statistical properties of the measured 30-min average meteorological and calculated variables with BREB.

Variables	Min	Max	Median	Average	Std. Deviation
T (°C)	-9.27	37.86	16.19	16.38	8.39
R _{Hmean} (%)	27.04	98.49	65.34	65.16	16.72
VPD (kPa)	0.02	4.51	0.60	0.85	0.79
R _S (W/m ²)	0	1039	464.1	478.5	273.4
ET _a (mm)	0	0.47	0.12	0.14	0.11

racy models can be obtained even by using only global solar radiation as the input.

The statistical features of the observed parameters used in this study are given in Tab. 2.

2.2 Support vector machine

Support vector machine (SVM) is a data-driven machine learning approach based on statistical learning theory. Although SVM was initially used to best distinguish between two classes of data, it was later developed with multiple classification studies for data requiring more than two classes. This separation is expected to be made as optimal as possible. To make the most appropriate classification, a linear decision surface, i.e. the

hyperplane, is constructed (Cortes and Vapnik, 1995). The hyperplane established in the space, maximizes the distance between the data of both classes. This distance is called a margin and maximizing margin is essential to minimize error. Besides, in determining the hyper-plane that separates the instance space linearly, only the marginal values have an effect, while changing the remaining samples does not have an effect on hyper-plane. The support vector machines model is implemented by moving the input vectors nonlinearly to a high dimensional space. The kernel functions are used for this process. For the nonlinear data, kernel functions greatly increase learning performance.

The structure of the support vector machines is shown in Fig. 4. In this method, the SVM has no information about the distribution of input data set. The attribute value of each input data, along with the value of a given coordinate, is plotted as a support vector in n-dimensional space. Decision planes are created for classification using these support vectors as training data and thereafter, it is able to classify input data sets with support vector machines separating the two classes. With this method, learning process is performed on input data and prediction is made.

Let $[(x_1, y_1), (x_2, y_2), (x_3, y_3), \dots, (x_n, y_n)]$ be a training set, where n denotes the number of training data set, x_i and y_i represent input and output vectors, respectively. The best function for the support vector regression as follows:

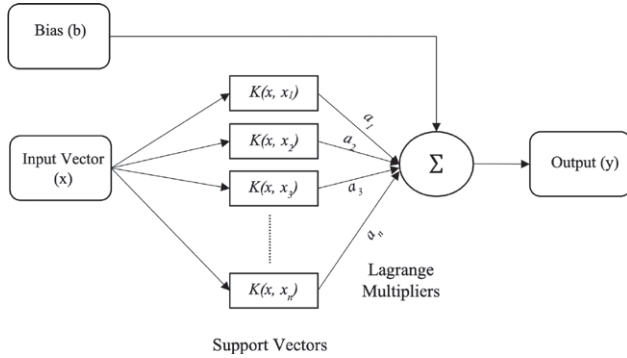


Fig. 4. Schematic view of the SVM structure.

$$f(x) = w \cdot \varphi(x) + b \quad (4)$$

in which, w represents the normal vector, b and $\varphi(x)$ are the bias term and the non-linear function, respectively. The objective function is the minimum of the $\varphi(x)$ as following:

$$\min \frac{1}{2} \|w\|^2 + c \sum_{i=1}^n (\xi_i + \xi_i^*) \quad (5)$$

Constraints:

$$\begin{aligned} y_i - w \cdot \varphi(x) - b &\leq \varepsilon_i + \xi_i \\ w \cdot \varphi(x) + b - y_i &\leq \varepsilon_i + \xi_i^* \\ \xi_i, \xi_i^* &\geq 0; i=1, 2, \dots, n \end{aligned} \quad (6)$$

C is the penalty parameter which provides stability to maximize margin range and minimize misclassification. ε is the insensitive loss function, ξ and ξ^* are slack variables denotes the upper and lower constraints on the system output, respectively. The insensitive loss function is a function that ignores the error at a certain distance from the target value. By using the Lagrange theory, the function can be expressed as:

$$f(x) = \text{sign} \left[\sum_{i=1}^n (a_i - a_i^*) K(x_i, x) + b \right] \quad (7)$$

where $K(x_i, x)$ is the Kernel function and a, a^* represents the Lagrange multipliers. Kernel function can be expressed as generally:

$$K(x, y) = \langle \varphi(x), \varphi(y) \rangle \quad (8)$$

In this study, the radial basis function (RBF) was used as kernel and the equation of RBF as follows:

$$K(x, y) = \exp\left(-\frac{\|x - y\|^2}{2\sigma^2}\right) \quad (9)$$

where σ denotes the radial basis function width. The parameters of SVM, C , ε and σ are selected by trial-error method.

2.3. Adaptive neuro fuzzy inference system

Fuzzy logic is an approach introduced by Zadeh (1965). It is based on expressing an object or phenomenon in a fuzzier manner, without sharp boundaries, rather than being expressed with precise values. This form of expression is called fuzzification. The fuzzified values are then processed in accordance with the rules set by the user and the desired modeling is performed. The process of converting model outputs to actual values is called defuzzification, and there are two commonly used types in the literature. The first inference type is Mamdani (1974) which can work with the help of verbal expressions and graphical operations. The second and the most widely used inference in engineering field is Takagi-Sugeno (1985) type inference system. This method is suitable for use with numerical values and clarifies fuzzy expressions with the help of a constant or linear equation. Today, the most commonly used structure of Takagi-Sugeno inference system is ANFIS. ANFIS can be described as the combination of fuzzy logic approach and artificial neural network learning algorithms (Jang 1993). The ANFIS algorithm is described in Fig. 5.

Layer 1: The data set values are fuzzified. For instance, ‘‘Less’’ and ‘‘Very’’ were used to express the input values divided into two sets. Therefore, the membership degree for the input value is determined as follows:

$$\mu_{A_i}(I_i) = \exp\left[-\left(\frac{I - c_i}{\sigma_i}\right)^2\right] \quad (10)$$

in which; I_i denotes the two fuzzy sets named as ‘‘Less’’ and ‘‘Very’’. c_i and σ_i refer to the parameters of the mem-

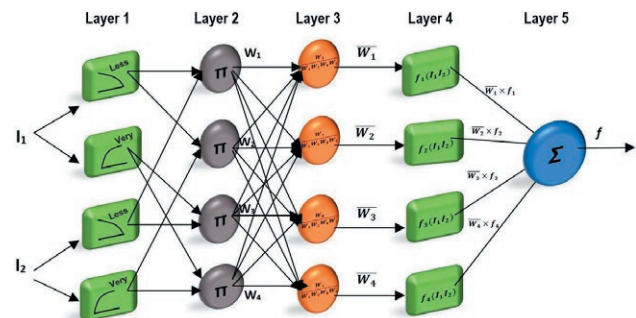


Fig. 5. Architecture of ANFIS model.

bership function, which will be optimized later, called the premise parameters.

Layer 2: By multiplying the membership degrees calculated in Layer 1, the output value of each node is obtained. The result will be named as firing strength:

$$w_i = \mu_{A_i}(I_1) \times \mu_{B_i}(I_2) \quad i=1,2,\dots \quad (11)$$

Layer 3: Using the input values of Layer 2, the normalized firing strength is calculated as follows:

$$\bar{w}_i = \frac{w_i}{\sum w_i} \quad i=1,2,\dots \quad (12)$$

Layer 4: Using the firing strength value from Layer 3, the correct equations representing the relationships are obtained. The so-called consequence parameters are calculated in Layer 4:

$$\bar{w}_i f_i = \bar{w}_i (p_i l_1 + q_i l_2 + r_i) \quad i=1,2,\dots \quad (13)$$

where p_i , q_i and r_i are the consequence parameters.

Layer 5: In the fifth layer, the final output value is obtained by summing all the values from the previous step. Besides, there is only one node in this layer.

$$f = \sum \bar{w}_i f_i \quad i=1,2,\dots \quad (14)$$

2.4. Artificial neural network

The application of ANN has continued to increase over the last few decades (Aghelpour *et al.*, 2019). Research in this area revealed that ANN plays a vital role in the modeling of parameters which have nonlinear behavior with low error. Firstly, in the 1940s, engineering studies were carried out (McCulloch and Pitts, 1943). When it comes to the 1960s, rapidly developing artificial neural network model studies entered the period of stagnation since the networks that can be used easily in solving linear problems could not solve nonlinear problems. Following the 1970s, there was a great explosion in the studies carried out in this field, starting with the comprehension of the abilities of ANN about solving non-linear problems (Rumelhart *et al.*, 1986). Today, artificial neural networks focused on the concept of “deep learning” (LeCun *et al.*, 2015). Considerable progress has been made in several fields of study, such as image processing (Indraswari *et al.*, 2019) and object recognition (Mhalla *et al.*, 2019). Complex structures can be solved very quickly, particularly with the increasing

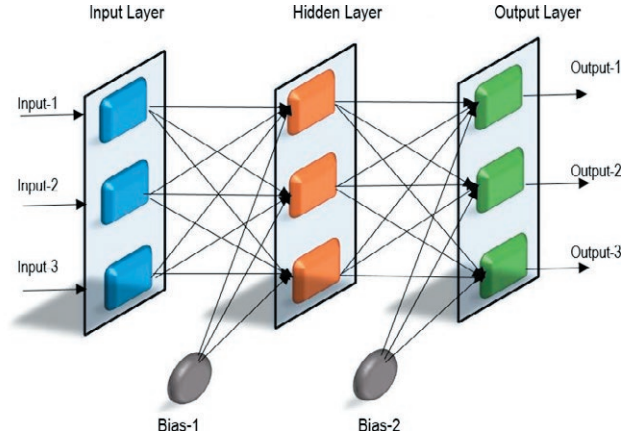


Fig. 6. Structure of the multi-layer perceptron.

of computer processor speeds. For the solution of non-linear problems, Rumelhart (1986) developed multi-layer artificial neural networks. Similar to the working principle of single-layer networks, multi-layer networks undergo a learning process by comparing the given input samples with the outputs. In the learning process, weights are obtained to minimize the difference between output and expected values.

Multilayer artificial neural networks consist of 3 layers, named as input layer, hidden layer, and output layer (Fig. 6).

Multilayer artificial neural networks work with the principle of supervised learning. In multi-layer perceptron (MLP), inputs and expected outputs should be given for the learning of the network and the network intends to compare the model output values with the expected output values in order to minimize the difference. MLP, performs this purpose with two types of calculation: (1) Feed Forward and (2) Back Propagation. The calculation steps are as follows:

1. The net input value obtained by multiplying the weights by the input values:

$$Net = \sum_i^n I_i W_i \quad (15)$$

2. The net input value is converted into the following equation via the activation function:

$$F(Net) = \frac{1}{1 + e^{-Net}} \quad (16)$$

where I and W represent input value and weights, respectively.

3. The output of the activation function from the hidden layer is re-weighted and the final output value is

reached by a linear transfer function in the output layer.

4. The final output value is compared with the expected values identified to the network. The comparison is performed by taking the difference between the expected value and the output generated by the network. At this stage, it is desired that the error sum of squares be zero. If it is far from zero, the weights must be re-updated in order to approach zero.

$$E = \frac{1}{2} \sum_i^n (E_i - O_i)^2 \quad (17)$$

where E_i and O_i denote expected and output values, respectively. From this step, backpropagation is carried out.

5. The gradient of the “E” value representing the error is taken to update the network weights. In each iteration, new values of weights are found and subtracted from the previous weight values.
6. If the change in the weight of the neuron connecting the i th element in the hidden layer to n th element in the output layer is A , the change in weight at time t is calculated as follows:

$$\Delta A_{in}^a = \lambda \delta_n C_i^a + \alpha \Delta A_{in}^a (t - 1) \quad (18)$$

where λ and α represent the learning coefficient and momentum coefficient, respectively. The momentum coefficient ensures that the amount of change is added to the next change at a constant rate, while preventing the network from getting stuck to the local minimum during the learning process. The learning coefficient determines how much change required to be in weights. δ_n is the error of the output and calculated as follows:

$$\delta_n = f'(Net)E \quad (19)$$

7. After determining the amount of change in weight, the value in t th iteration is calculated with the help of the Equation 6.

$$A_{in}^a(t) = A_{in}^a(t - 1) + \Delta A_{in}^a(t) \quad (20)$$

8. Updating the weights of the threshold values also be carried out with the aid of Equation 20.

2.6. Performance evaluation criteria

In data driven models, a number of metrics are used to evaluate model performances. With the help of these metrics, statistical comparisons are made and it is con-

cluded whether the model results are statistically significant or not. In this study, mean absolute error (MAE), mean squared error (MSE), Nash-Sutcliffe Efficiency (NSE), Performance index (PI) and Willmott’s refined index of agreement (WI) were employed in the model evaluation (Nash and Sutcliffe, 1970). All the metrics used have different ability to measure the closeness of model results and observations. Therefore, a fair comparison can be achieved by using those metrics.

Nash-Sutcliffe Efficiency (NSE) varies between $-\infty$ and 1. If the efficiency value is 1, then it means that the model has a perfect match with observations.

$$NSE = 1 - \frac{\sum_{i=1}^n (D_{oi} - D_{pi})^2}{\sum_{i=1}^n (D_{oi} - \bar{D}_o)^2} \quad (21)$$

Where D_o is observed values, D_p is predicted values and \bar{D}_o is the average of observed values. Performance Index (PI) varies between 0 and ∞ . If the PI values are close to zero, then the model has high accuracy (Gandomi and Roke 2015).

$$PI = \frac{RMSE/\bar{D}_o}{1 + \frac{\sum_{i=1}^n [(D_{oi} - \bar{D}_o)(D_{pi} - \bar{D}_p)]}{\sqrt{\sum_{i=1}^n (D_{oi} - \bar{D}_o)^2 \sum_{i=1}^n (D_{pi} - \bar{D}_p)^2}}} \quad (22)$$

Willmott’s refined index of agreement (WI) varies between -1 and 1. Likewise NSE, the model can be defining as successful if the WI value approaches to 1. If the WI value is -1, model interpretation should be performed carefully (Willmott *et al.* 2012).

$$WI=1 - \frac{\sum_{i=1}^n |D_{pi} - D_{oi}|}{c \times \sum_{i=1}^n |D_{oi} - \bar{D}_o|}, \text{ when}$$

$$\sum_{i=1}^n |D_{pi} - D_{oi}| \leq c \times \sum_{i=1}^n |D_{oi} - \bar{D}_o|; \text{ (with } c=2) \quad (23a)$$

$$WI=1 - \frac{c \times \sum_{i=1}^n |D_{oi} - \bar{D}_o|}{\sum_{i=1}^n |D_{pi} - D_{oi}|} - 1, \text{ when}$$

$$\sum_{i=1}^n |D_{pi} - D_{oi}| > c \times \sum_{i=1}^n |D_{oi} - \bar{D}_o|; \text{ (with } c=2) \quad (23b)$$

Coefficient of determination (R^2) value varies between -1 and 1, just the same way as WI. Positive values indicate that two variables are directly proportional, while negative values represent the inverse relationship. Approaching to -1 or 1 increases the strength of the relationship, whereas in the case of zero, it means that there is no relationship between the variables. MSE and MAE

are both expected to be close to zero and the equations are given as follows:

$$MSE = \frac{1}{n} \sum_{i=1}^n (D_{pi} - D_{oi})^2 \quad (24)$$

$$MAE = \frac{1}{n} \sum_{i=1}^n |D_{pi} - D_{oi}| \quad (25)$$

3. RESULTS AND DISCUSSION

In this study, three different data-driven methods, named as support vector machines, adaptive-network-based fuzzy inference system and artificial neural networks were used to estimate 30-min actual evapotranspiration values. In this context, the field measurement of various climatic variables that are used in the calculation of evapotranspiration has been carried out, and estimations have been made depending on these parameters. Thus, global solar radiation, relative humidity, mean temperature and vapor pressure deficit were used as input variables to the proposed models, while actual ET as the output. To achieve the parsimonious selection of the most effective inputs, first of all single input-output models were tried by taking each variable separately as an input (Tab. 3). Then the accuracy of the multiple input – single output models were compared with the results of the single input – single output models by increasing the number of inputs to the proposed models in each time. Additionally, the separation of the data set, which is one of the most influencing factors on the model accuracy, was performed as 70% training set and 30% test set.

3.1. SVM results

In the training phase of models that use SVM method, data were transformed to a different space to per-

form linear separation due to the nonlinear nature of the data. For this process, there are four different kernel functions used in the literature: (1) linear, (2) polynomial, (3) sigmoid, and (4) radial based function (RBF). The choice of the kernel functions depends on user's preferences, as well as the data structure. The structure of natural phenomena is generally non-linear and contains chaotic behavior. For this reason, the RBF is the most preferred function by researchers since it has ability to generalize the bounds on the probability of classification error. Therefore, RBF was used in the present study. There are three parameters that need to be optimized for Radial Basis Function (RBF) kernel SVM. Those parameters are called as gamma, penalty parameter (C) and epsilon. Here, the parameters were optimized using-trial error method.

First, single input – single output models were obtained as reference models, then multiple input – single output models were built. The abbreviations SVM1, SVM2, SVM3 and SVM4 represent the models built by using mean temperature, relative humidity, vapor pressure deficit and solar radiation as an input, respectively. The results obtained by the SVM models revealed that the SVM4 model which uses the solar radiation variable as a single input has the highest accuracy among all single input-single output models. The SVM4 model has the determination coefficient as $R^2=0.909$, while the rest of the models have lower than the $R^2=0.5$. The model performance started to improve as the number of inputs increase in the model setup. For instance, SVM5 and SVM6 models perform better ($NSE_{SVM5} = 0.9387$, $NSE_{SVM6} = 0.9163$), and SVM7 model that uses all of the four input variables, shows highest prediction performance ($NSE_{SVM7} = 0.9398$). It is observed that multiple input - single output SVM models deviate slightly from the perfect model line (Fig. 7). The SVM4 model performance is considered to be quite satisfactory when compared to the SVM7 model event if its error criteria is slightly less than the SVM7. The evaluation of the SVM models with

Tab. 3. Models identities and corresponding input variables.

	Methods			INPUTS	OUTPUT
	SVM	ANFIS	ANN		
Model IDs	SVM1	ANFIS1	ANN1	T	ET _a
	SVM2	ANFIS2	ANN2	R _H	ET _a
	SVM3	ANFIS3	ANN3	VPD	ET _a
	SVM4	ANFIS4	ANN4	R _S	ET _a
	SVM5	ANFIS5	ANN5	T, R _S	ET _a
	SVM6	ANFIS6	ANN6	T, R _H , R _S	ET _a
	SVM7	ANFIS7	ANN7	T, R _H , R _S , VPD	ET _a

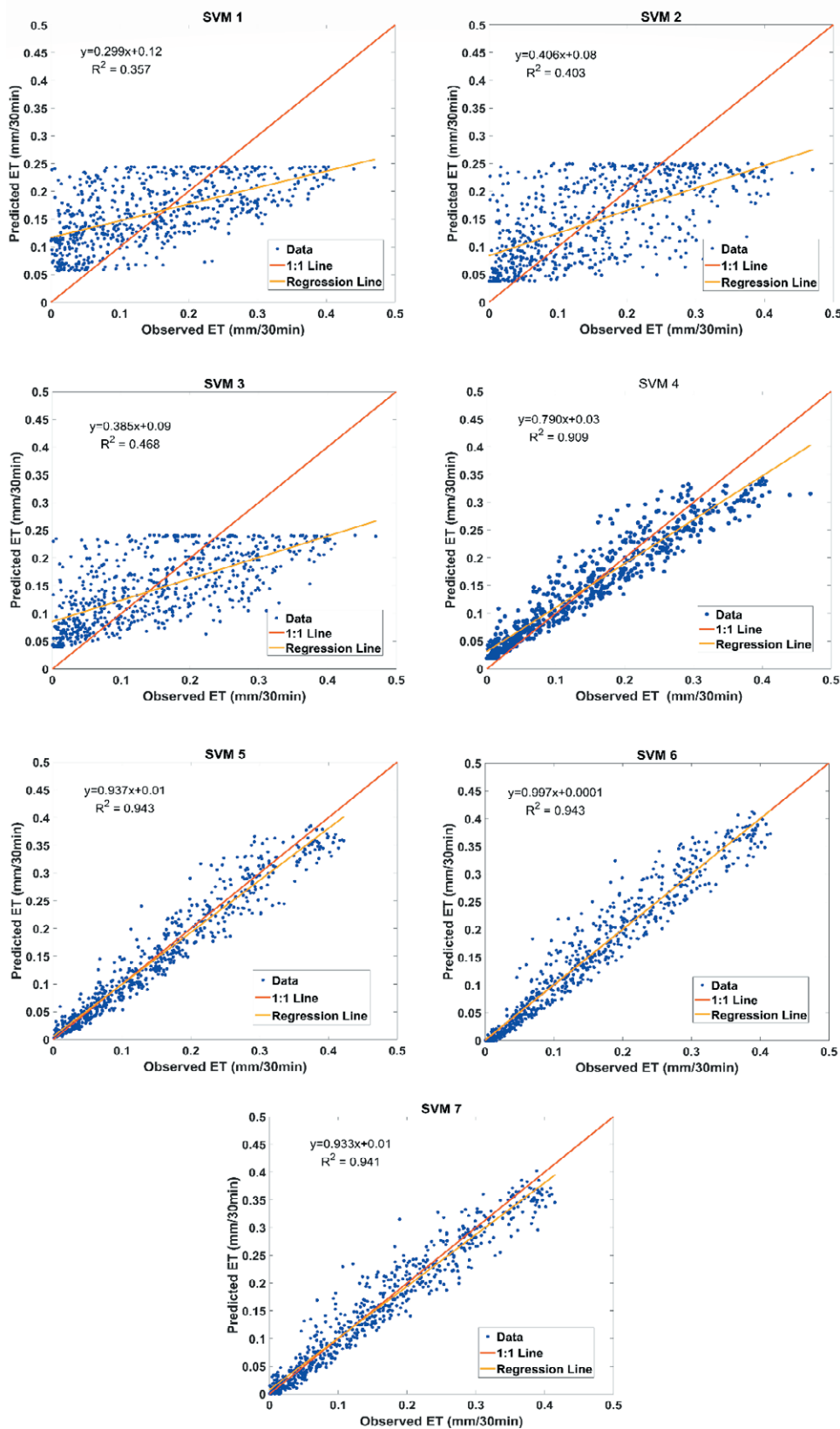


Fig. 7. Scatter plots of SVM models for testing data.

respect to different performance indicators is given in the Tab. 4.

3.2. ANFIS results

ANFIS models were built by using fuzzy logic toolbox found in MATLAB software. Triangle, trapezoidal and gaussian type membership functions were used for the different model setups. Using trial and error method, it is found that the models with gaussian type membership function has the lowest training error. Therefore, gaussian type member function was employed for the ANFIS model to predict the ET_a values in testing part. The number of fuzzy sets, which is selected based on expert opinion, is another parameter encountered during the training phase. In this study, the number of fuzzy sets which can be between 2 and 5 was determined by trial and error method. Although a training error decreases as the number of fuzzy sets increase, it may cause over-learning to select too many membership functions. Since overlearning would reduce the generalization ability of the models, generally upper limit is taken as five membership functions depending on time series length. Three fuzzy sets were found to be adequate to achieve the best ANFIS model performances in training part.

In the Sugeno inference type, the output values can be in the form of either a constant number or a linear equation. This option is selected by the user and does not have any significant impact on our current results. So, it is decided to use linear equations for a better generalization. The parameters of linear equation were calculated with least squares method, the membership function parameters were obtained by back propagation algorithm. These training methods readily built in Matlab ANFIS editor under the “hybrid” option. ANFIS7 model, which has 4 inputs, gave the best prediction accuracy for the testing data set, among the models established by ANFIS. On the other hand, the single input-single output models, except ANFIS4 model, yield lower prediction performance ($NSE_{ANFIS1}=0.308$, $MAE_{ANFIS1}=0.075$; $NSE_{ANFIS2}=0.392$, $MAE_{ANFIS2}=0.067$; $NSE_{ANFIS3}=0.4658$, $MAE_{ANFIS3}=0.061$) compared to multiple input-single output models ($NSE_{ANFIS5}=0.928$, $MAE_{ANFIS5}=0.022$; $NSE_{ANFIS6}=0.935$, $MAE_{ANFIS6}=0.021$; $NSE_{ANFIS7}=0.941$, $MAE_{ANFIS7}=0.0198$). Also, ANFIS4 model gave considerably successful results according to the performance metrics, such as MAE, MSE, NSE, WI and PI with 0.025, 0.001, 0.907, 0.866 and 0.113 respectively. Even tough, the accuracy of multiple input-single output models is better than the ANFIS4 model, the results are considered to be close to each other and successful pre-

dictions can be made with solar radiation (R_s), particularly in the cases where limited data exists.

The results show that the ANFIS model that has the same input combination gives very close NSE and MSE values to the SVM model. In other words, the actual ET values predictions were achieved with a high accuracy using a single input solar radiation both in the SVM and ANFIS model. The NSE, MSE, WI and PI values of each ANFIS model are given in Table 4. Moreover, the scatter plot of the models created with only solar radiation revealed a good scattering which can be considered as useful (Fig. 8).

3.3. ANN results

Multilayer perceptron (MLP) have been used in the application of ANN. As a first step, input and output data were normalized. The normalization is the de-unitization process, which enables the use of data in different scales within the same model. Normalization was performed by dividing all values by the time series' maximum values, which can be called also as idealization. Thus, values for all data set are reduced between 0 and 1. The neural network architecture consists of three layers which are (1) input layer, (2) hidden layer and (3) output layer. Sigmoid, tangent-hyperbolic and step functions, which are not only mostly used for the solution of the non-linear problems but also the most common transfer functions in the literature, were evaluated to use in the hidden layer. The tangent-hyperbolic function (THF) was chosen, because of its best performance results. The number of hidden neurons was evaluated in the range of 3 to 5 by trial and error method. Since the number of neurons 15 and/or above 15 is thought to lead to over-learning and will result in complex model structure, the number of hidden neurons is restricted to 15. Backpropagation was chosen as the training algorithm and learning coefficient and momentum coefficients were selected as 0.001 and 0.5, respectively. Considering the evaluations carried out according to different performance metrics, it is concluded that the ANN5 (the model with 2 inputs, named as T_{mean} and R_s) has the highest accuracy with $NSE = 0.946$ and $MSE = 7E-4$. Besides, with a slight difference between each other, ANN6 and ANN7 models were obtained as the second and third best models, respectively ($NSE_{ANN6}=0.942$, $MSE_{ANN6}=8E-4$; $NSE_{ANN7}=0.941$, $MSE_{ANN7}=8E-4$).

On the other hand, ANN4 model, which was generated by using only R_s as an input, has the best estimation performance among the single input single output models with $NSE = 0.91$ and $MSE = 11E-4$. Considering that there is not much difference between the results according

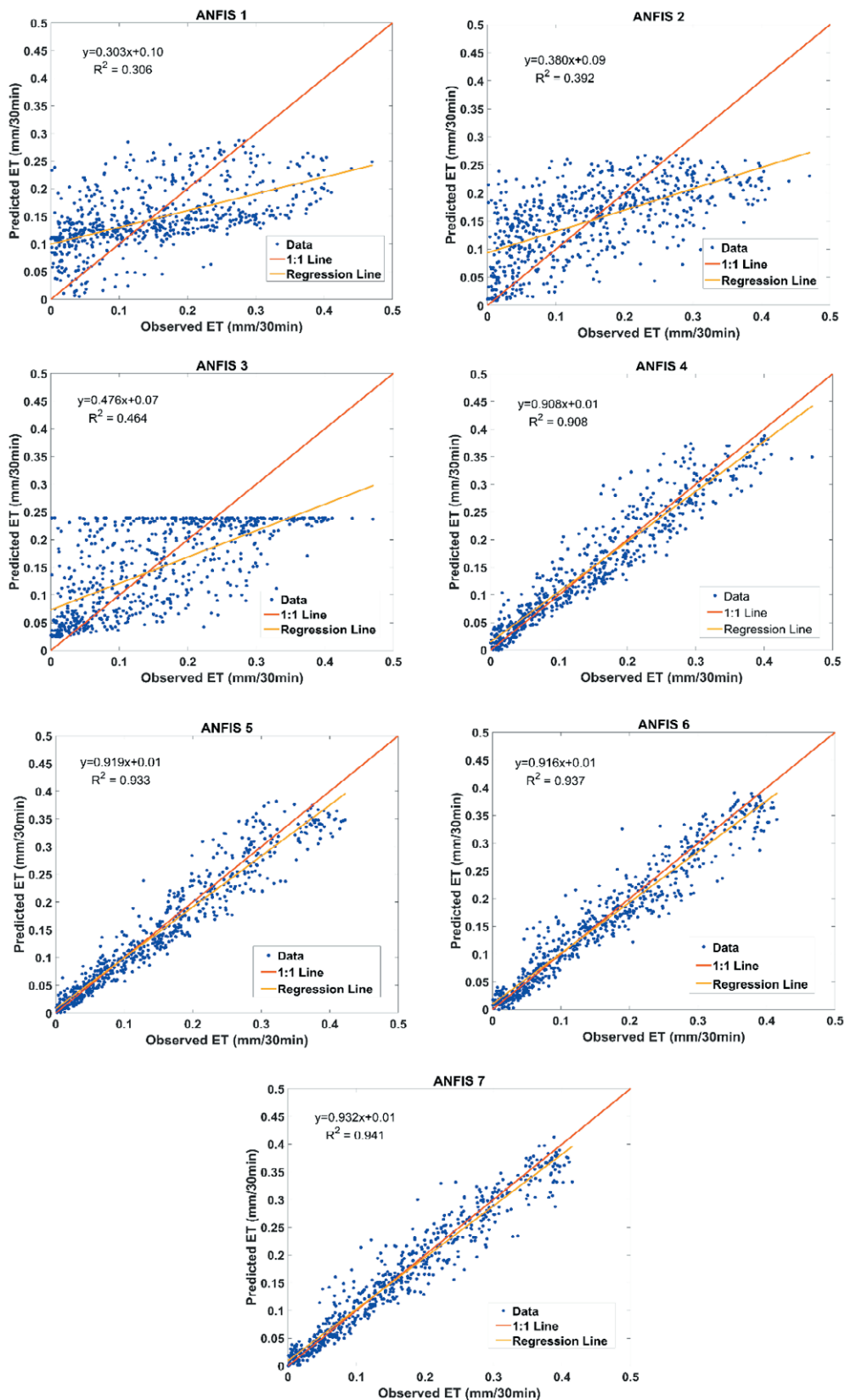


Fig. 8. Scatter plots of ANFIS models for testing data.

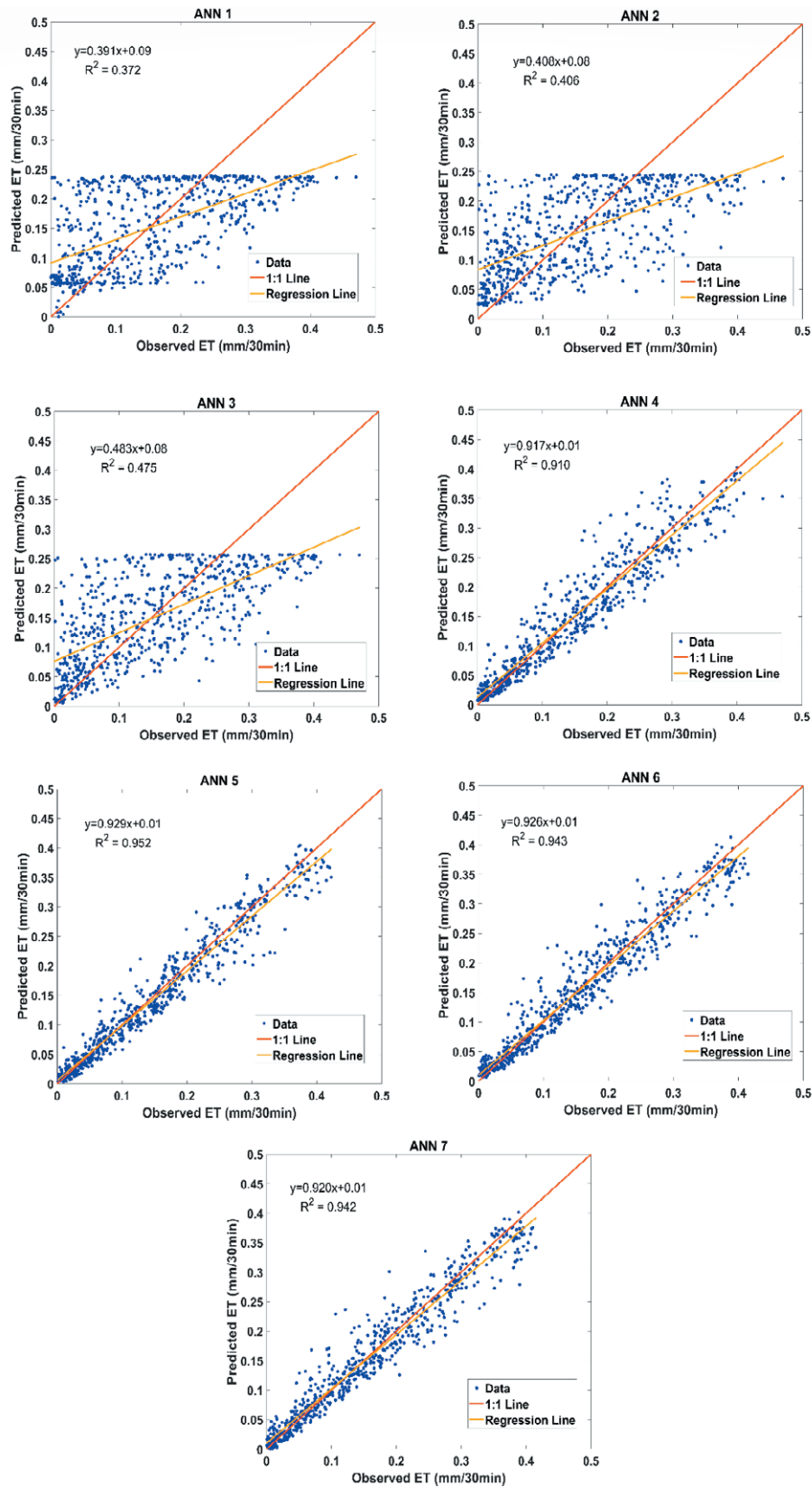


Fig. 9. Scatter plots of ANN models for testing data.

to the performance indicators, the actual ET values can be estimated at high success rate by using solely measured R_s with the help of ANN4. Model structures and prediction performances of ANN are also given in Table 4.

The scattering plots of the models established with ANN are shown in Fig. 9. ANN4, ANN5, ANN6 and ANN7 models distributed on a 1:1 perfect model line, while ANN1, ANN2 and ANN3 deviate highly from the perfect model line. Also, it indicates that the ANN4 model is not underestimated or overestimated and can be preferred in prediction of ET_a values as an alternative for the multiple input - single output models with a slight difference in the model accuracies.

As can be seen from the box plot diagrams given in Fig. 10, error distribution range for single input - single output data-driven models, except the models which only solar radiation was used as an input, can be considered as high, in comparison to the multiple input - single output data-driven models' error distributions. There are extreme error values for single input - single output data-driven models, while weights of negative and positive values tend to be relatively equal in the distribution of error values for the multiple input - single output data-driven models, as well as the models which only solar radiation was used as an input. The box plots also present that the errors of the data-driven models are distributed as close to zero. Consequently, it can be said that although multiple input - single output models provide relatively better performances, the model with global solar radiation as an input appears to be considerably successful in terms of practical use with that requires only one variable.

4. CONCLUSION

Today, with inadequate clean water resources, the large amount of water used in agricultural irrigation and the increasing evaporation rate, ET calculations have gained importance for the effective use of water resources. In this article, data-based models were used to evaluate ET_a values measured by BREB method. Throughout the study, the prediction of the measured ET_a values with different and limited meteorological variables, which are temperature, relative humidity, global solar radiation and vapor pressure difference, was performed. According to the obtained results of the study, the prediction performances of the models which are created using only global solar radiation (R_s) as an input were very close to the performance of the multiple input-single output models created using all other meteorological inputs. The main findings of the study are as follows:

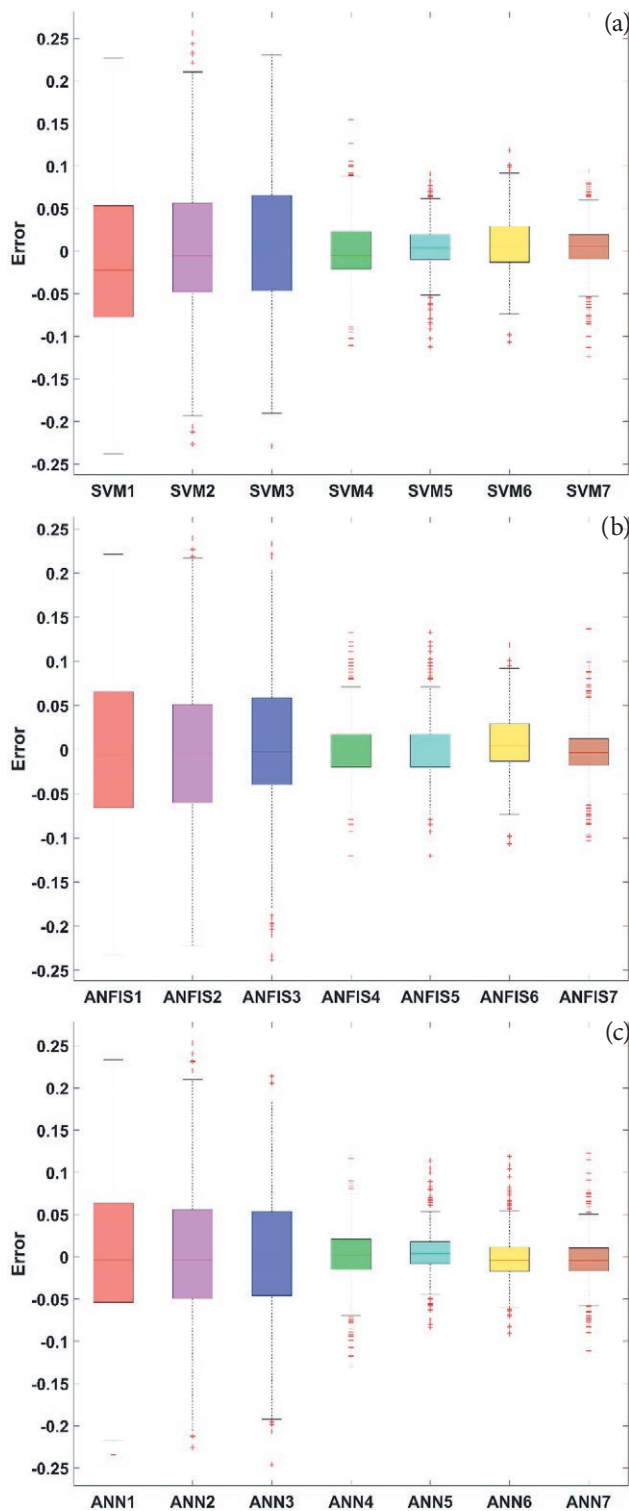


Fig. 10. Box plots of the models' error values for testing data. (a) SVM models (b) ANFIS models (c) ANN models.

Tab. 4. Performances of All Models.

Method Model	Inputs	Output	TRAIN					TEST					
			MAE	MSE	NSE	WI	PI	MAE	MSE	NSE	WI	PI	
SVM	1	T	ET _a	0.0749	0.0079	0.346	0.598	0.381	0.0741	0.0078	0.3407	0.6009	0.3686
	2	R _H	ET _a	0.0678	0.0073	0.399	0.636	0.359	0.0066	0.0071	0.4012	0.6426	0.3435
	3	VPD	ET _a	0.0640	0.0065	0.468	0.656	0.325	0.0645	0.0065	0.4527	0.6523	0.3187
	4	R _S	ET _a	0.0272	0.0013	0.8971	0.8539	0.1243	0.0277	0.0013	0.8938	0.8508	0.1213
	5	T, R _S	ET _a	0.0211	0.0008	0.9297	0.8864	0.1013	0.0204	0.0008	0.9387	0.8908	0.0936
	6	T, R _H , R _S	ET _a	0.0240	0.0010	0.9169	0.8686	0.1114	0.0251	0.0011	0.9163	0.8704	0.1062
	7	T, R _H , R _S , VPD	ET _a	0.0202	0.0008	0.9341	0.8896	0.0991	0.0207	0.0008	0.9398	0.8930	0.0900
ANFIS	1	T	ET _a	0.0753	0.0084	0.3059	0.5956	0.4062	0.0749	0.0082	0.3081	0.5962	0.3884
	2	R _H	ET _a	0.0695	0.0075	0.3797	0.6269	0.3690	0.0674	0.0072	0.3923	0.6367	0.3485
	3	VPD	ET _a	0.0602	0.0061	0.5012	0.6766	0.3132	0.0615	0.0063	0.4658	0.6685	0.3155
	4	R _S	ET _a	0.0241	0.0010	0.9142	0.8706	0.1134	0.0249	0.0011	0.9073	0.8659	0.1134
	5	T, R _S	ET _a	0.0222	0.0009	0.9253	0.8803	0.1045	0.0222	0.0009	0.9277	0.8814	0.1019
	6	T, R _H , R _S	ET _a	0.0203	0.0008	0.9328	0.8888	0.1001	0.0209	0.0008	0.9359	0.8920	0.0929
	7	T, R _H , R _S , VPD	ET _a	0.0180	0.0006	0.9450	0.9016	0.0903	0.0198	0.0008	0.9410	0.8974	0.0890
ANN	1	T	ET _a	0.0701	0.0075	0.3847	0.6237	0.3667	0.0694	0.00746	0.3762	0.6260	0.3559
	2	R _H	ET _a	0.0672	0.0073	0.4025	0.6390	0.3583	0.0660	0.0071	0.4044	0.6444	0.3426
	3	VPD	ET _a	0.0604	0.0061	0.4975	0.6760	0.3150	0.6094	0.0062	0.4794	0.6717	0.3100
	4	R _S	ET _a	0.0236	0.0010	0.9157	0.8735	0.1125	0.0240	0.0011	0.9096	0.8710	0.1119
	5	T, R _S	ET _a	0.0194	0.0007	0.9383	0.8956	0.0946	0.0185	0.0007	0.9459	0.9011	0.0877
	6	T, R _H , R _S	ET _a	0.0199	0.0008	0.9351	0.8909	0.0983	0.0203	0.0008	0.9422	0.8952	0.0881
	7	T, R _H , R _S , VPD	ET _a	0.0197	0.0007	0.9369	0.8922	0.0969	0.0201	0.0008	0.9409	0.8960	0.0891

- The application of data-driven models such as SVM, ANFIS and ANN models showed that data-driven mathematical methods can yield easier and faster solutions in ET predictions.
- It is concluded that in cases of limited facilities in the measurement of climatic variables, it is possible to make accurate ET_a calculations by using only global solar radiation.

In addition, unlike the other studies that a few performance metrics were employed to measure their model accuracies, a variety of performance metrics were used in this paper. This led to a fairer evaluation of model performances. Also, the accuracy of the models established using limited meteorological variables was highlighted, while well accepted predictions were obtained using only global solar radiation as an input.

ACKNOWLEDGEMENTS

The data used in this study was obtained from the project (109R006) supported by the Scientific and Technological Research Council of Turkey (TÜBİTAK). Therefore, we would like to thank TÜBİTAK for finan-

cial support of the project. In addition, special thanks to Dr. Fatih Bakanoğulları and the technicians who helped us during the experimental studies at Atatürk Soil Water and Agricultural Meteorology Research Institute for their contributions.

REFERENCES

- Abdullah, S.S., Malek, M.A., Abdullah, N.S., Kisi, O., Yap, K.S. 2015. Extreme Learning Machines: A new approach for prediction of reference evapotranspiration. *Journal of Hydrology*, <https://doi.org/10.1016/j.jhydrol.2015.04.073>
- Aghelpour, P., Mohammadi, B., Biazar, S.M. 2019. Long-term monthly average temperature forecasting in some climate types of Iran, using the models SARI-MA, SVR, and SVR-FA. *Theoretical and Applied Climatology*, <https://doi.org/10.1007/s00704-019-02905-w>
- Ahmed, K., Sachindra, D.A., Shahid, S., Iqbal, Z., Nawaz, N., Khan, N. 2020. Multi-model ensemble predictions of precipitation and temperature using machine learning algorithms. *Atmospheric Research*, <https://doi.org/10.1016/j.atmosres.2019.104806>

- Allen, R.G., Pereira, L.S., Raes, D., Smith, M. 1998. Crop evapotranspiration —guidelines for computing crop water requirements. FAO Irrigation and drainage paper 56. Food and Agriculture Organization, Rome.
- Antonopoulos, V.Z., Antonopoulos, A. V. 2017. Daily reference evapotranspiration estimates by artificial neural networks technique and empirical equations using limited input climate variables *Computers and Electronics in Agriculture*, <https://doi.org/10.1016/j.compag.2016.11.011>
- Banda, P., Cemek, B., Küçüktopcu, E. 2018. Estimation of daily reference evapotranspiration by neuro computing techniques using limited data in a semi-arid environment. *Archives of Agronomy and Soil Science*, <https://doi.org/10.1080/03650340.2017.1414196>
- Bowen, I.S. 1926. The ratio of heat losses by conduction and by evaporation from any water surface. *Physical Review*. 27, 779-787.
- Cortes, C., Vapnik, V. 1995. Support-Vector Networks. *Machine Learning* <https://doi.org/10.1023/A:1022627411411>
- Ekmekyapar, F., Cebi, U.K. 2017. An investigation of inorganic chemicals and heavy metals in Kırklareli dam water, thrace region. *Desalination and Water Treatment*, <https://doi.org/10.5004/dwt.2017.21316>
- Elkiran, G., Nourani, V., Abba, S.I. 2019. Multi-step ahead modelling of river water quality parameters using ensemble artificial intelligence-based approach. *Journal of Hydrology*, <https://doi.org/10.1016/j.jhydrol.2019.123962>
- Fan, J., Yue, W., Wu, L., Zhang, F., Cai, H., Wang, X., Lu, X., Xiang, Y. 2018. Evaluation of SVM, ELM and four tree-based ensemble models for predicting daily reference evapotranspiration using limited meteorological data in different climates of China. *Agricultural and Forest Meteorology*, <https://doi.org/10.1016/j.agrformet.2018.08.019>
- Ferreira, L.B., da Cunha, F.F., de Oliveira, R.A., Fernandes Filho, E.I. 2019. Estimation of reference evapotranspiration in Brazil with limited meteorological data using ANN and SVM – A new approach. *Journal of Hydrology*, <https://doi.org/10.1016/j.jhydrol.2019.03.028>
- Gandomi, A.H., Roke, D.A. 2015. Assessment of artificial neural network and genetic programming as predictive tools. *Advances in Engineering Software*, <https://doi.org/10.1016/j.advengsoft.2015.05.007>
- Gocic, M., Petković, D., Shamshirband, S., Kamsin, A. 2016. Comparative analysis of reference evapotranspiration equations modelling by extreme learning machine. *Computers and Electronics in Agriculture*, <https://doi.org/10.1016/j.compag.2016.05.017>
- Indraswari, R., Kurita, T., Arifin, A.Z., Suciati, N., Astuti, E.R. 2019. Multi-projection deep learning network for segmentation of 3D medical images. *Pattern Recognition Letters*, <https://doi.org/10.1016/j.patrec.2019.08.003>
- Jang, J.R. 1993. ANFIS: adaptive-network-based fuzzy inference system. *IEEE Transactions on Systems, Man, and Cybernetics: Systems*, <https://doi.org/10.1109/21.256541>.
- Khaledi, C.K.A. 2019. Projection of harvestable water from air humidity using artificial neural network (Case study: Chabahar Port). *Italian Journal of Agrometeorology*. 24 (1), 3-11.
- Lazzus, J. A. 2014. Estimation of surface soil temperature based on neural network modeling. *Italian Journal of Agrometeorology*. 19 (2), 5-12.
- LeCun, Y., Bengio, Y., Hinton, G. 2015 Deep learning. *Nature* <https://doi.org/10.1038/nature14539>
- Liu, L., Gao, C., Xuan, W., Xu, Y.P. 2017. Evaluation of medium-range ensemble flood forecasting based on calibration strategies and ensemble methods in Lanjiang Basin, Southeast China. *Journal of Hydrology*, <https://doi.org/10.1016/j.jhydrol.2017.08.032>
- Mamdani, E.H. 1974. Application of Fuzzy Algorithms for Control of Simple Dynamic Plant. *Proceedings of the Institution of Electrical Engineers*, <https://doi.org/10.1049/piee.1974.0328>
- Maroufpoor S., Bozorg-Haddad O., Maroufpoor E. 2020. Reference evapotranspiration estimating based on optimal input combination and hybrid artificial intelligent model: Hybridization of artificial neural network with grey wolf optimizer algorithm. *Journal of Hydrology* 588:125060. <https://doi.org/10.1016/j.jhydrol.2020.125060>
- McCulloch, W.S., Pitts, W. 1943. A logical calculus of the ideas immanent in nervous activity. *Bulletin of Mathematical Biophysics*, <https://doi.org/10.1007/BF02478259>
- Mhalla, A., Chateau, T., Amara, N.E. Ben. 2019. Spatio-temporal object detection by deep learning: Video-interlacing to improve multi-object tracking. *Image and Vision Computing* <https://doi.org/10.1016/j.imavis.2019.03.002>
- Nash, J.E. and Sutcliffe, J.V. 1970. River Flow Forecasting through Conceptual Model. Part 1—A Discussion of Principles. *Journal of Hydrology*, [http://dx.doi.org/10.1016/0022-1694\(70\)90255-6](http://dx.doi.org/10.1016/0022-1694(70)90255-6)
- Nourani, V., Elkiran, G., Abdullahi, J. 2019. Multi-station artificial intelligence based ensemble modeling of reference evapotranspiration using pan evaporation measurements. *Journal of Hydrology*, <https://doi.org/10.1016/j.jhydrol.2019.123958>

- Ohmura, A. 1982. Objective criteria for rejecting data for Bowen ratio flux. *Journal of Applied Meteorology and Climatology*. 21, 595-583 598.
- Partalas, I., Tsoumakas, G., Hatzikos, E. V., Vlahavas, I. 2008. Greedy regression ensemble selection: Theory and an application to water quality prediction. *Information Sciences* <https://doi.org/10.1016/j.ins.2008.05.025>
- Penman, H.L. 1948. Natural Evaporation from Open Water, Bare Soil and Grass. *Proceedings of the Royal Society of London*, <https://doi.org/10.1098/rspa.1948.0037>
- Perez, P.J. Castellvi, F., Ibañez, M., Rosell, J.I. 1999. Assessment of reliability of Bowen ratio method for partitioning fluxes. *Agricultural and Forest Meteorology*, 97, 141-150.
- Rumelhart, D.E., Hinton, G.E., Williams, R.J. (1986) Learning representations by back-propagating errors. *Nature*, <https://doi.org/10.1038/323533a0>
- Şaylan, L., Kimura, R., Çaldağ, B., Akataş, N. 2017. Modeling of soil water content for vegetated surface by artificial neural network and adaptive neuro-fuzzy inference system. *Italian Journal of Agrometeorology*. 22 (3), 37-44.
- Şaylan, L., Kimura, R. Altınbas, N., Çaldağ, B., Bakanoğulları, F. 2019. Modeling of Surface Conductance over Sunn Hemp by Artificial Neural Network, *Italian Journal of Agrometeorology*, 24, 3, 37-48.
- Takagi, T., Sugeno, M. 1985. Fuzzy Identification of Systems and Its Applications to Modeling and Control. *IEEE Transactions on Systems, Man, and Cybernetics: Systems*. <https://doi.org/10.1109/TSMC.1985.6313399>
- Tiwari, M.K., Chatterjee, C. 2010. Uncertainty assessment and ensemble flood forecasting using bootstrap based artificial neural networks (BANNs). *Journal of Hydrology*, <https://doi.org/10.1016/j.jhydrol.2009.12.013>
- Turc, L. 1961. Water requirements assessment of irrigation, potential evapotranspiration: Simplified and updated climatic formula. *Annales Agronomiques*, 12, 13-49.
- Wen, X., Si, J., He, Z., Wu, J., Shao, H., Yu, H. 2015. Support-Vector-Machine-Based Models for Modeling Daily Reference Evapotranspiration with Limited Climatic Data in Extreme Arid Regions *Water Resources Management*, <https://doi.org/10.1007/s11269-015-0990-2>
- Willmott, C.J., Robeson, S.M., Matsuura, K. 2012. A refined index of model performance. *International Journal of Climatology*, <https://doi.org/10.1002/joc.2419>
- Wu, L., Zhou, H., Ma, X., Junliang, F., Zhang., F. 2019. Daily reference evapotranspiration prediction based on hybridized extreme learning machine model with bio-inspired optimization algorithms: Application in contrasting climates of China. *Journal of Hydrology*. 577:123960. <https://doi.org/10.1016/j.jhydrol.2019.123960>
- Xu, L., Chen, N., Zhang, X., Chen, Z. 2020. A data-driven multi-model ensemble for deterministic and probabilistic precipitation forecasting at seasonal scale. *Climate Dynamics*. <https://doi.org/10.1007/s00382-020-05173-x>
- Yassin, M.A., Alazba, A.A., Mattar, M.A. 2016. Artificial neural networks versus gene expression programming for estimating reference evapotranspiration in arid climate. *Agricultural Water Management*. <https://doi.org/10.1016/j.agwat.2015.09.009>
- Zadeh, L.A. 1965. Fuzzy Sets. *Information and Control*, 8, 338-353.